Electronic Supplementary Information for Dalton Transactions

Synthesis and Characterization of Aryl Substituted *Bis*(2-pyridyl)amines and their Copper Olefin Complexes: Investigation of Remote Steric Control over Olefin Binding†

John J. Allen, Christopher E. Hamilton, and Andrew R. Barron*

Energy and Environmental Systems Institute and Department of Chemistry,

Rice University, Houston, Texas 77005, USA

Supplementary Material (ESI)

N-[(2-isopropyl)phenyl]-N-(2-pyridyl)amine (1). FTIR (neat, ATR, cm^{-1}): 3201 (w, ν_{N-H}), 3161 (w), 3091 (w, aromatic ν_{C-H}), 3008 (w, aromatic ν_{C-H}), 2954 (w, alkyl ν_{C-H}), 2859 (w, alkyl ν_{C-H}), 1584 (s), 1529 (s), 1450-1329 (s, aromatic $\delta_{C=C}$), 1150 (m), 1083 (m), 1033 (m), 993 (m). ^{13}C NMR ($CDCl_3$): δ 157.86, 147.94, 143.81, 138.29, 136.94, 126.81, 126.65, 126.10, 125.59, 114.40, 107.37, 28.12, 23.46.

N-mesityl-N,N-(2,2'-dipyridyl)amine (2). FTIR (neat, ATR, cm^{-1}): 3150 (w, aromatic ν_{C-H}), 3068 (w, aromatic ν_{C-H}), 3048 (w, aromatic ν_{C-H}), 3004 (w, aromatic ν_{C-H}), 2972 (w, alkyl ν_{C-H}), 2916 (w, alkyl ν_{C-H}), 2854 (w, alkyl ν_{C-H}), 1584 (s), 1563 (m), 1463-1319 (s, aromatic $\delta_{C=C}$), 1257 (m, aromatic $\delta_{C=N}$), 1147 (s), 988 (s). ^{13}C NMR (CD_3OD): δ 158.03, 148.74, 139.79, 139.74, 139.24, 138.49, 131.23, 119.01, 116.43, 21.28, 18.66.

N-(2,6-diethylphenyl)-N,N-(2,2'-dipyridyl)amine (3). FTIR (neat, ATR, cm^{-1}): 3151 (w, aromatic ν_{C-H}), 3069 (w, aromatic ν_{C-H}), 3048 (w, aromatic ν_{C-H}), 3003 (w, aromatic ν_{C-H}), 2972 (w, alkyl ν_{C-H}), 2956 (w, alkyl ν_{C-H}), 2911 (w, alkyl ν_{C-H}), 2877 (w, alkyl ν_{C-H}), 1618 (m), 1584 (s), 1561 (m), 1465-1319 (s, aromatic $\delta_{C=C}$), 1279 (m, aromatic $\delta_{C=N}$), 1150 (m), 987 (m). ^{13}C NMR (298 K; $CDCl_3$): δ 157.11, 148.24, 143.28, 140.36, 137.35, 128.44, 127.21, 117.17, 114.76, 24.43, 13.90.

N-(2-isopropylphenyl)-N,N-(2,2'-dipyridyl)amine (4). FTIR (neat, ATR, cm^{-1}): 3054 (w, aromatic ν_{C-H}), 3005 (w, aromatic ν_{C-H}), 2959 (m, alkyl ν_{C-H}), 2922 (w, alkyl ν_{C-H}), 2866 (w, alkyl ν_{C-H}), 1583 (s), 1569 (s), 1463-1316 (s, aromatic $\delta_{C=C}$), 1277 (s, aromatic $\delta_{C=N}$), 1150(s), 1083 (m), 989 (m), 867 (w). ^{13}C NMR (CD_3OD): δ 159.36, 148.83, 148.77, 142.76, 139.58, 131.43, 129.61, 129.00, 128.82, 119.32, 117.75, 29.28, 23.91.

N-(2,6-diisopropylphenyl)-N,N-(2,2'-dipyridyl)amine (5). FTIR (neat, ATR, cm^{-1}): 3178 (w, aromatic ν_{C-H}), 3057 (w, aromatic ν_{C-H}), 3008 (w, aromatic ν_{C-H}), 2959 (w, alkyl ν_{C-}

$_H$), 2926 (w, alkyl ν_{C-H}), 2867 (w, alkyl ν_{C-H}), 1595 (m), 1584 (s), 1527 (m), 1467-1328 (s, aromatic $\delta_{C=C}$), 1255 (m, aromatic $\delta_{C=N}$), 1147(m), 989 (m). ^{13}C NMR ($CDCl_3$): δ 157.45, 148.13, 148.00, 138.45, 137.23, 129.03, 124.92, 117.12, 114.99, 28.67, 23.94.

N-(1-naphthyl)-N,N-(2,2'-dipyridyl)amine (6). FTIR (neat, ATR, cm^{-1}): 3129 (w, aromatic ν_{C-H}), 3074 (w, aromatic ν_{C-H}), 3044 (w, aromatic ν_{C-H}), 2992 (w, aromatic ν_{C-H}), 2975 (w, aromatic ν_{C-H}), 2910 (w), 1583 (s), 1559 (m), 1462-1314 (s, aromatic $\delta_{C=C}$), 1267 (m, aromatic $\delta_{C=N}$), 1151 (m), 990 (m). ^{13}C NMR ($CDCl_3$): δ 158.14, 148.30, 137.87, 135.45, 131.61, 128.76, 128.17, 127.87, 127.13, 126.62, 126.53, 123.78, 117.88, 115.98.

(N-mesityl-N,N-(2,2'-dipyridyl)amine)hydrogen tetrafluoroborate (7). FTIR (neat, ATR, cm^{-1}): 3104 (w, aromatic ν_{C-H}), 3063 (w, aromatic ν_{C-H}), 2941 (w, alkyl ν_{C-H}), 2921 (w, alkyl ν_{C-H}), 2859 (w, alkyl ν_{C-H}), 2736 (w, vb), 1634 (w), 1593 (s), 1527 (m), 1458-1367 (s, aromatic $\delta_{C=C}$), 1292 (m), 1253 (m, aromatic $\delta_{C=N}$), 1164 (m), 1032 (vs), 769 (vs). ^{13}C NMR (CD_3OD): δ 154.51, 144.89, 143.25, 142.88, 138.10, 133.36, 132.55, 120.40, 114.93, 21.38, 17.32.

(N-(2-isopropyl)phenyl-N,N-(2,2'-dipyridyl)amine)hydrogen tetrafluoroborate (8). FTIR (neat, ATR, cm^{-1}): 3106 (w, aromatic ν_{C-H}), 3061 (w, aromatic ν_{C-H}), 2965 (w, alkyl ν_{C-H}), 2928 (w, alkyl ν_{C-H}), 2870 (w, alkyl ν_{C-H}), 2600 (vw, vb), 1639 (w), 1594 (s), 1527 (s), 1491-1370 (s, aromatic $\delta_{C=C}$), 1296 (m), 1257 (m, aromatic $\delta_{C=N}$), 1169 (m), 1032 (vs), 768 (vs). ^{13}C NMR (CD_3OD): δ 155.60, 148.89, 144.12, 142.92, 136.03, 133.05, 130.87, 130.76, 130.66, 120.30, 116.27, 29.21, 24.03.

Bis[N-(phenyl)-N,N-(2,2'-dipyridyl)amine]-dichloro-bis(μ-chloro)dicopper(II) (9). FTIR (neat, ATR, cm^{-1}): 3106 (w, aromatic ν_{C-H}), 3075 (w, aromatic ν_{C-H}), 3061 (w, aromatic

ν_{C-H}), 3039 (w, aromatic ν_{C-H}), 3021 (w, aromatic ν_{C-H}), 1600 (s), 1589 (s), 1566-1317 (s, aromatic $\delta_{C=C}$), 1274 (s, aromatic $\delta_{C=N}$), 1160 (m), 1053 (m), 1029 (m), 936 (m), 787 (s).

Bis[N-(2-isopropyl)phenyl-N,N-(2,2'-dipyridyl)amine]-dichloro-bis(μ-chloro)dicopper(II) (10). FTIR (neat, ATR, cm^{-1}): 3582 (w, ν_{O-H}), 3487 (w, ν_{O-H}), 3114 (w, aromatic ν_{C-H}), 3081 (w, aromatic ν_{C-H}), 3059 (w, aromatic ν_{C-H}), 3045 (w, aromatic ν_{C-H}), 3014 (w, aromatic ν_{C-H}), 1595 (s), 1578 (s), 1485-1321 (s, aromatic $\delta_{C=C}$), 1261 (m, aromatic $\delta_{C=N}$), 1248 (m), 1164 (m), 1060 (m), 1024 (m), 922 (m), 803 (m), 768 (vs).

Bis(N-(1-naphthyl)-N,N-(2,2'-dipyridyl)amine)-dichloro-bis(μ-chloro)dicopper(II) (11). FTIR (neat, ATR, cm^{-1}): 3582 (w, ν_{O-H}), 3487 (w, ν_{O-H}), 3114 (w, aromatic ν_{C-H}), 3081 (w, aromatic ν_{C-H}), 3059 (w, aromatic ν_{C-H}), 3045 (w, aromatic ν_{C-H}), 3014 (w, aromatic ν_{C-H}), 1595 (s), 1578 (s), 1485-1321 (s, aromatic $\delta_{C=C}$), 1261 (m, aromatic $\delta_{C=N}$), 1248 (m), 1164 (m), 1060 (m), 1024 (m), 922 (m), 803 (m), 768 (vs).

Bis(N-(mesityl)-N,N-(2,2'-dipyridyl)amine)-di-aquo-bis(μ-hydroxo)dicopper(II) bis(tetrafluoroborate) (12). FTIR (neat, ATR, cm^{-1}): 3532 (w, ν_{O-H}), 3197 (br, w), 3124 (w, aromatic ν_{C-H}), 3091 (w, aromatic ν_{C-H}), 3041 (w, aromatic ν_{C-H}), 2975 (w, alkyl ν_{C-H}), 2939 (w, alkyl ν_{C-H}), 2858 (w, alkyl ν_{C-H}), 2828 (w, alkyl ν_{C-H}), 1597 (s), 1580 (m), 1487-1327 (s, aromatic $\delta_{C=C}$), 1238 (m, aromatic $\delta_{C=N}$), 1027 (br, vs), 931 (w), 856 (w).

[Cu(Ph-dpa)(η^2-styrene)]BF_4 (13). FTIR (neat, ATR, cm^{-1}): 3136 (w, aromatic ν_{C-H}), 3102 (w, aromatic ν_{C-H}), 3079 (w, alkene ν_{C-H}), 3056 (w, alkene ν_{C-H}), 3037 (w, alkene ν_{C-H}), 1596 (s), 1572-1430 (s, aromatic $\delta_{C=C}$), 1328 (s), 1237 (m, aromatic $\delta_{C=N}$), 1063-1021 (br vs). ^{13}C NMR (298 K; CD_3OD): δ 157.10, 150.21, 143.48, 142.14, 138.70, 132.15, 129.94, 129.52, 129.11, 128.61, 127.18, 121.44, 120.35, 116.06 (H_2C=*C*H), 89.69 (H_2*C*=CH), 58.42 (O*C*H_2CH_3), 18.50 (OCH_2*C*H_3).

[Cu(Mes-dpa)(η^2-styrene)]BF_4 (14). FTIR (neat, ATR, cm^{-1}): 3100 (w, aromatic ν_{C-H}), 3077 (w, alkene ν_{C-H}), 3026 (w, alkene ν_{C-H}), 2982 (w, alkyl ν_{C-H}), 2918 (w, alkyl ν_{C-H}), 2858 (w, alkyl ν_{C-H}), 1598 (s), 1580-1426 (s, aromatic $\delta_{C=C}$), 1329 (s), 1233 (m, aromatic $\delta_{C=N}$), 1164 (m), 1046 (br vs). ^{13}C NMR (298 K; CD_3OD): δ 155.49, 150.62, 142.23, 141.80, 138.64, 138.07, 137.54, 132.40, 130.12, 129.29, 127.11, 119.80, 116.26, 104.60 (H_2C=*C*H), 77.28 (H_2*C*=CH), 21.31 (*p*-*C*H_3), 17.78 (*o*-*C*H_3).

[Cu{(2-^{i}Pr)Ph}-dpa)(η^2-styrene)]BF_4 (15). FTIR (neat, ATR, cm^{-1}): 3126 (w, aromatic ν_{C-H}), 3079 (w, alkene ν_{C-H}), 3060 (w, alkene ν_{C-H}), 3033 (w, alkene ν_{C-H}), 2967 (m, alkyl ν_{C-H}), 2927 (w, alkyl ν_{C-H}), 2871 (w, alkyl ν_{C-H}), 1600 (s), 1580-1430 (s, aromatic $\delta_{C=C}$), 1335 (s), 1233 (m, aromatic $\delta_{C=N}$), 1245 (s), 1055 (br vs), 1020 (br vs). ^{13}C NMR (298 K; CD_3OD): δ 156.76, 150.32, 148.45, 141.62, 139.81, 138.66, 132.58, 131.99, 130.62, 130.17, 129.74, 129.31, 127.12, 120.06, 118.05, 106.32 (H_2C=*C*H), 79.07 (H_2*C*=CH), 29.17, 23.73.

[Cu(naph-dpa)(η^2-styrene)]BF_4 (16). FTIR (neat, ATR, cm^{-1}): 3563 (m), 3167 (vw, aromatic ν_{C-H}), 3096 (w, aromatic ν_{C-H}), 3058 (w, alkene ν_{C-H}), 3028 (w, alkene ν_{C-H}), 2976 (w, alkyl ν_{C-H}), 2884 (w, alkyl ν_{C-H}), 1598 (s), 1578-1390 (s, aromatic $\delta_{C=C}$), 1330 (s), 1245 (m, aromatic $\delta_{C=N}$), 1165 (s), 1043 (br vs). ^{13}C NMR (298 K; CD_3OD): δ 157.13, 150.03, 141.70, 138.83, 138.73, 137.13, 131.88, 131.72, 130.56, 130.15, 129.75, 129.60, 129.36, 128.69, 128.04, 127.27, 123.22, 120.31, 118.30, 109.85 (H_2C=*C*H), 82.77 (H_2*C*=CH).

[Cu(Mes-dpa)(η^2-norbornylene)]PF_6 (17) FTIR (neat, ATR, cm^{-1}): 3678 (m), 3595 (m), 3128 (w, aromatic ν_{C-H}), 3105 (w, aromatic ν_{C-H}), 3015 (w, alkene ν_{C-H}), 2978 (w, alkene ν_{C-H}), 2933 (w, alkyl ν_{C-H}), 2872 (w, alkyl ν_{C-H}), 2860 (w, alkyl ν_{C-H}), 1600 (m), 1579-1429 (s, aromatic $\delta_{C=C}$), 1337 (s), 1244 (m), 1226 (m), 1170 (m), 1024 (w), 822 (br vs), 772 (s). ^{13}C

NMR (298 K; CD_3OD): δ 155.48, 153.60, 142.82, 142.01, 141.22, 138.06, 132.75, 119.95, 116.54, 103.75 (*C*H=*C*H), 44.32, 44.07, 25.61, 21.35, 17.59.

[Cu{(2-^{i}Pr)Ph}-dpa)(η^2-norbornylene)]BF_4 (18) FTIR (neat, ATR, cm^{-1}): 3635 (m), 3547 (m), 3127 (w, aromatic ν_{C-H}), 3080 (w, aromatic ν_{C-H}), 3058 (w, alkene ν_{C-H}), 3031 (w, alkene ν_{C-H}), 2967 (w, alkyl ν_{C-H}), 2927 (w, alkyl ν_{C-H}), 2871 (w, alkyl ν_{C-H}), 1600 (s), 1582-1430 (s, aromatic $\delta_{C=C}$), 1334 (s), 1245 (m), 1055 (br vs), 1023 (br, vs), 780 (s). ^{13}C NMR (298 K; CD_3OD): δ 156.63, 150.71, 141.85, 138.07, 132.31, 132.17, 130.78, 130.73, 130.15, 119.92, 118.18, 103.87 (*C*H=*C*H), 44.31, 44.07, 29.11, 25.60, 23.82.

Special structural refinement details. Compound **3** was found to crystallize with two unique molecules in the asymmetric unit. Structure solution and refinement was performed in the asymmetric space group monoclinic $P2_1$, with TWIN/BASF instructions. Friedel pairs were merged (MERG 4) for refinement. Molecule 2 of the asymmetric unit is shown in Figure S1, and a comparison of the two comformers is shown in Figure S2.

Compound **4** crystallized with 2 unique molecules in the asymmetric unit, one of which exhibited a site occupancy disorder of the isopropyl methyl groups. The disordered methyl carbon atoms were given different PART numbers, and were refined as having a 50:50 site occupancy disorder. Unless otherwise noted, for each compound having a disorder present, the site occupancies were determined using the free variable (FVAR) command for the different parts. Initial refinement cycles were performed with fixed-distance restraints (DFIX 1.53) for all C(36)-C(methyl) bond lengths and (DANG 2.48) for corresponding C(methyl)-C(methyl) distances. Methyl hydrogen atoms were placed in idealized positions for a disordered methyl group (HFIX 123). Restraints were lifted for final refinement cycles. Structure solution and refinement was performed in the asymmetric space group orthorhombic $Pna2_1$, with TWIN/BASF instructions. Friedel pairs were merged (MERG 4) for refinement. The disorder in

molecule 2 of the asymmetric unit is shown below in Figure S3, and a comparison of the two comformers is shown in Figure S4.

Compound **5** was found to crystallize with 2 unique molecules in the asymmetric unit. Molecule 2 of the asymmetric unit is shown below in Figure S5, and a comparison of the two comformers is shown in Figure S6.

The BF_4^- anion present in the crystal structure of **7** was found to have a 75:25 site occupancy disorder for three of the four fluorine atoms. The disorder, shown below in Figure S7, is a C_2 rotation about the axis of the B(1)-F(1) bond. For initial refinement cycles, similar distance restraints (SADI) were placed on all B-F and F-F distances, in addition to similar ADP restraints (SIMU) and rigid bond restraints (DELU) for all F atoms. Restraints were lifted for final refinement cycles.

The BF_4^- anion present in the crystal structure of **8** was found to have a 50:50 site occupancy disorder for all four fluorine atoms. The disorder, shown below in Figure S8, is a C_2 rotation slightly tilted off the axis of the B(1)-F(1A) bond. Refinement was carried out in a similar manner to that in compound **7**. Use of the program PLATON revealed solvent accessible voids in the lattices of **8**, **15**, and **16**, and use of the SQUEEZE function led to better agreement of data in each case.

Crystal packing in compound **9** (Figure S9) reveals π-π stacking between pyridyl rings of adjacent molecules, having 3.654(1) Å between ring centers and a 0º mean plane angle difference. The crystal lattice of compound **11** was found to contain a solvent molecule of MeOH within H-bonding distance [O(1S)···Cl(2) = 3.20(1) Å] of the non-bridging Cl atom (see Figure S10). A more intricate H-bonding network was observed in packing of **12** (Fig S11) between copper-bound H_2O and OH^- ligands, MeOH solvent molecules, and BF_4^- anions. The BF_4^- anion present in **12** was found to have a 60:40 site occupancy disorder of the four fluorine atoms. The disorder, shown below in Figure S12, is a C_2 rotation slightly tilted off the axis of the B(1)-F(1A) bond. Refinement of the disorder was carried out in a similar manner to that in compound **8**.

The disordered BF_4^- anion present in the crystal structure of **13** was refined in a similar manner to that of compound **8**, having 50:50 site occupancies about a C_2 rotation slightly tilted off the B(1)-F(2A) bond (Fig S13). Crystal packing in **13** (Fig S14) shows a number of intermolecular interactions, including Cu···Ph_{sty} π-interaction, py···py' π-stacking in adjacent molecules. Moreover, Cu···O and hydrogen-bonding interactions with the BF_4^- anion were observed with an ethanol solvent of crystallization molecule.

Compound **14** was found to crystallize with 2 unique molecules in the asymmetric unit. Molecule 2 of the asymmetric unit is shown below in Figure S15, and a comparison of the two comformers is shown in Figure S16. Both BF_4^- anions exhibited 50:50 site occupancy disorders, the first is a C_2-rotation tilted off the B(1)-F(4A) bond, while the second is disordered about an inversion centered on the boron atom. Refinement was carried out similarly to the aforementioned cases, with the exception that fixed distance restraints for nonbonded atoms (DANG) were left in place for disordered fluorines attached to B(2) (Figure S17). An approximate isotropic behavior restraint (ISOR) on C(47) was also left in place for final refinement.

The disordered BF_4^- anion in **15** exhibits a 65:35 site occupancy disorder for three of the four fluorine atoms about a C_2-rotation along the B(1)-F(1) bond. Refinement of the disorder was performed similarly to that in compound **7**, with the exception that only SADI and DELU restraints were lifted in final refinement cycles (Figure S18).

Compound **16** was found to crystallize with 2 unique molecules in the asymmetric unit. Molecule 2 of the asymmetric unit is shown below in Figure S19. Comparison of the conformers can be found in the discussion section of the text.

The PF_6^- anion in compound **17** exhibits a 50:50 site occupancy disorder for four of the six fluorine atoms about a C_4-rotation along the F(1)-P(1)-F(2) vector (Figure S20). The H-bonding interaction between this anion and the MeOH solvent of crystallization is shown in Figure S21.

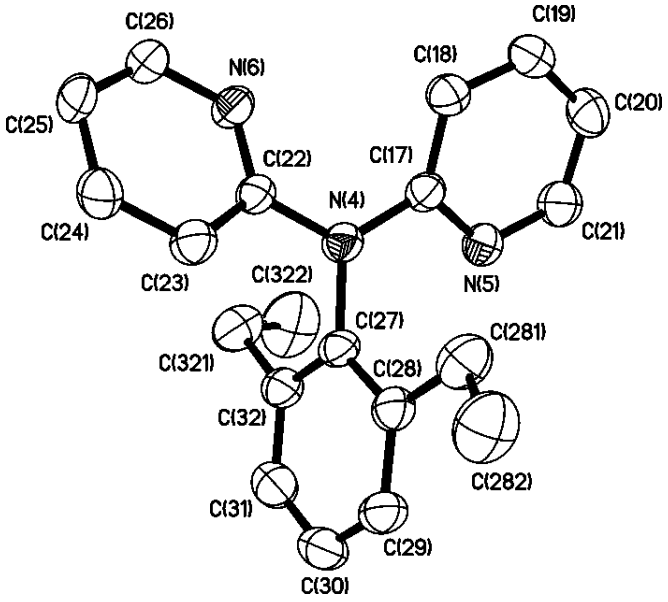

Fig. S1. Molecular structure of the second unique molecule present in the asymmetric unit of compound **3**. Thermal ellipsoids are shown at the 30% level, and all hydrogen atoms are omitted for clarity.

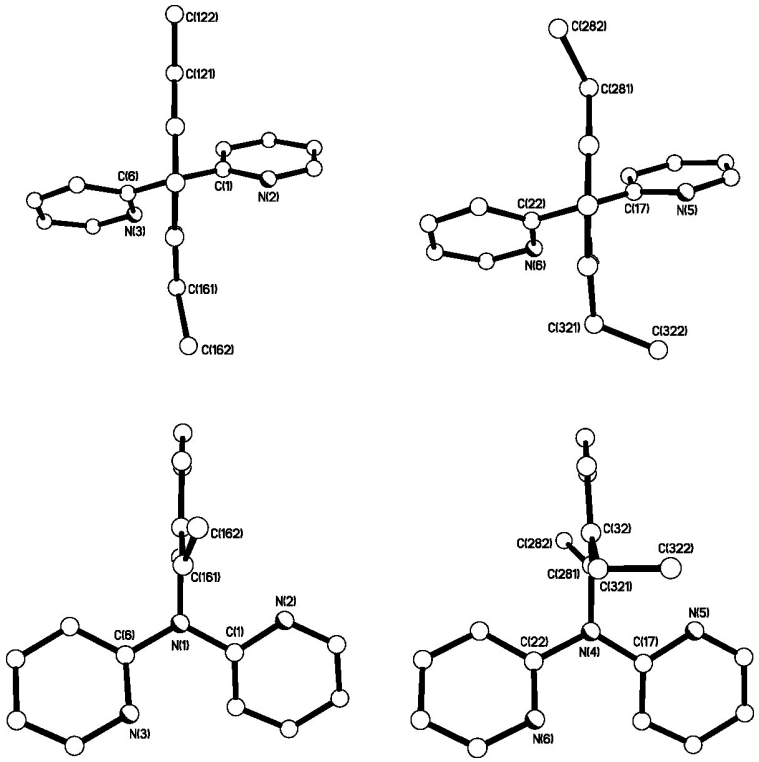

Fig. S2. Comparison of unique conformers present in the asymmetric unit of compound **3**.

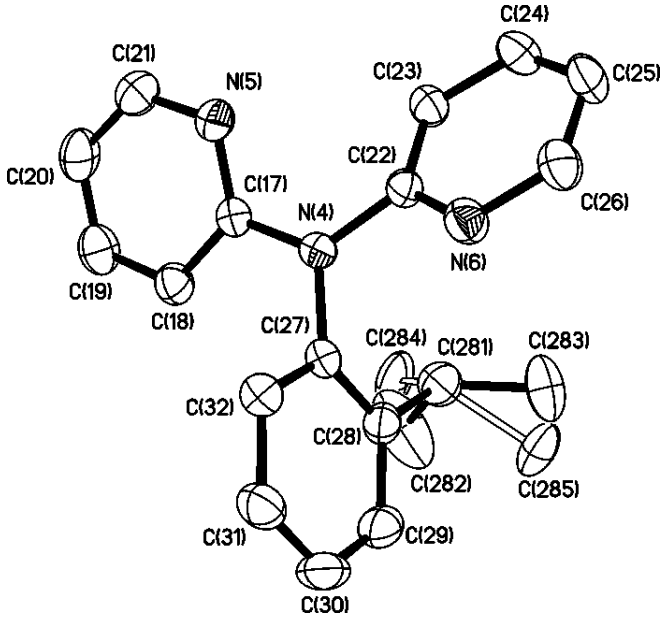

Fig. S3. Molecular structure of the second unique molecule present in the asymmetric unit of compound **4**. Thermal ellipsoids are shown at the 30% level, and all hydrogen atoms are omitted for clarity.

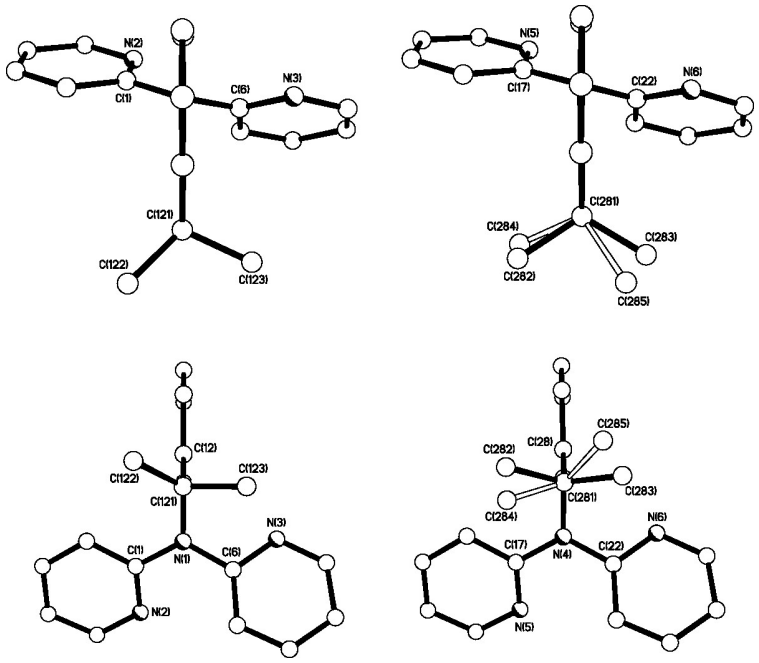

Fig. S4. Comparison of unique conformers present in the asymmetric unit of compound **4**.

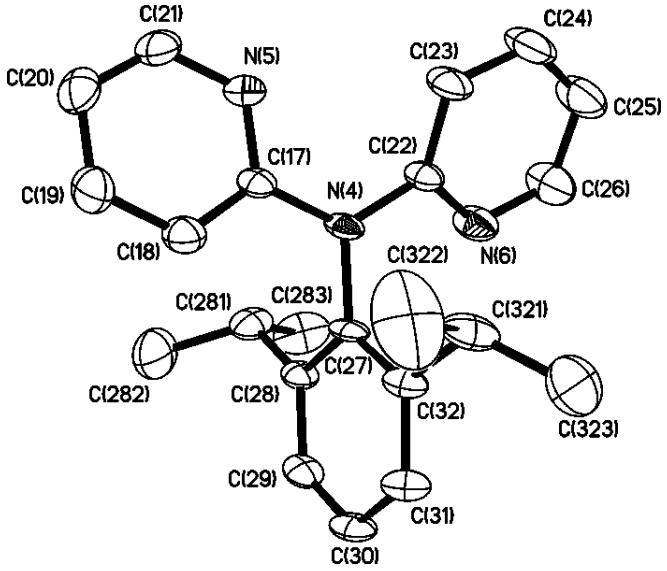

Fig. S5. Molecular structure of the second unique molecule present in the asymmetric unit of compound **5**. Thermal ellipsoids are shown at the 30% level, and all hydrogen atoms are omitted for clarity.

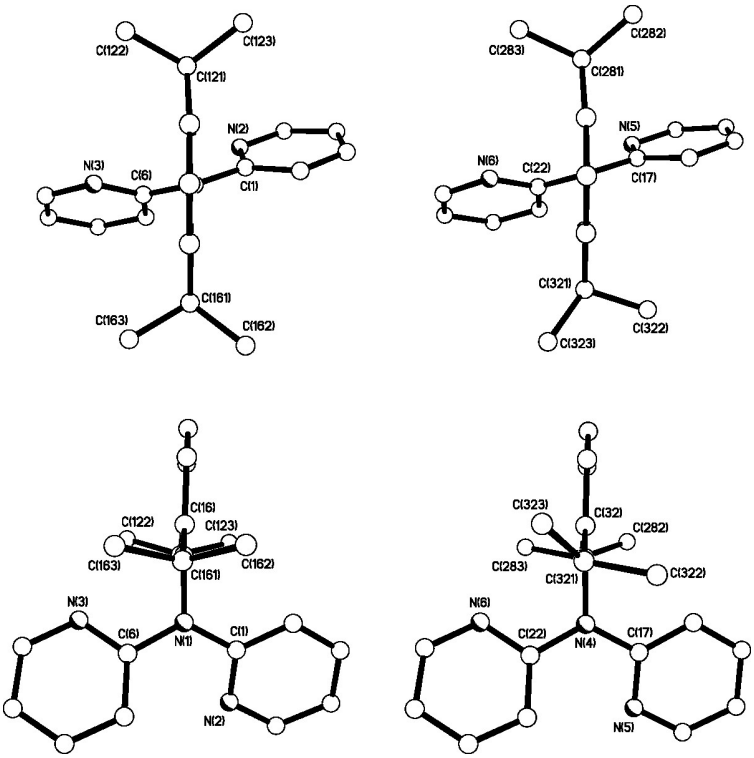

Fig. S6. Comparison of unique conformers present in the asymmetric unit of compound **5**.

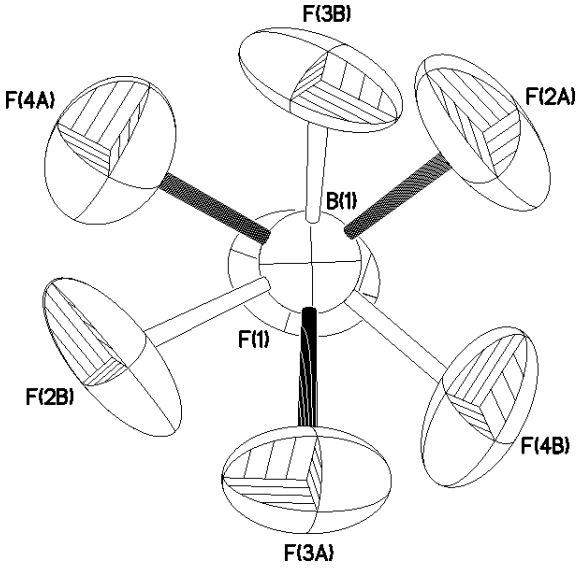

Fig. S7. Structure for the BF_4^- anion in compound **7** with both parts of the disorder present. For clarity, thermal ellipsoids are shown at the 20 % level.

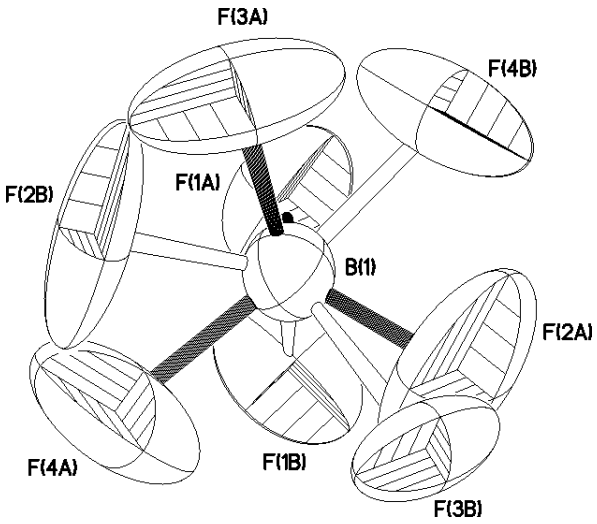

Fig. S8. Structure for the BF_4^- anion in compound **8** with both parts of the disorder present. For clarity, thermal ellipsoids are shown at the 20 % level.

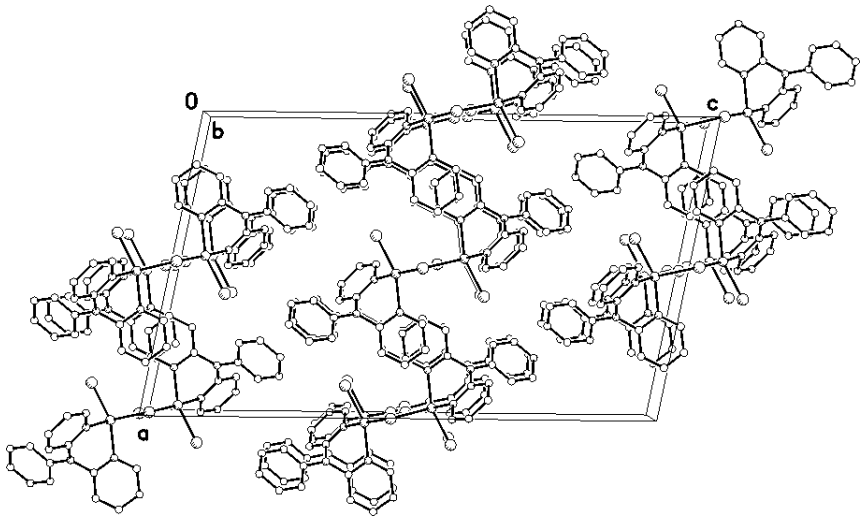

Fig. S9 Molecular packing diagram of **9** viewed along the b-axis, showing π-π stacking interaction between pyridyl rings of adjacent molecules. All hydrogen atoms are omitted for clarity.

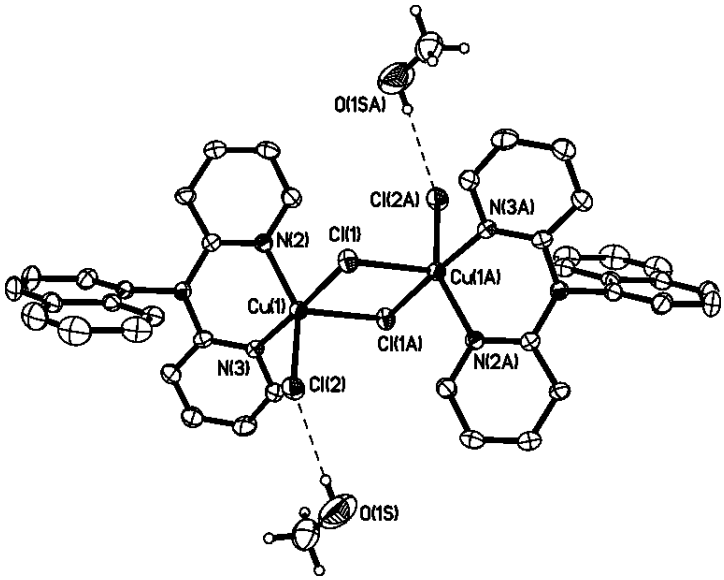

Fig. S10. Molecular structure of **11** showing location of MeOH solvent molecules found in the crystal lattice. Thermal ellipsoids are shown at the 30% level, and for clarity, only hydrogen atoms attached to the MeOH solvent molecules are shown.

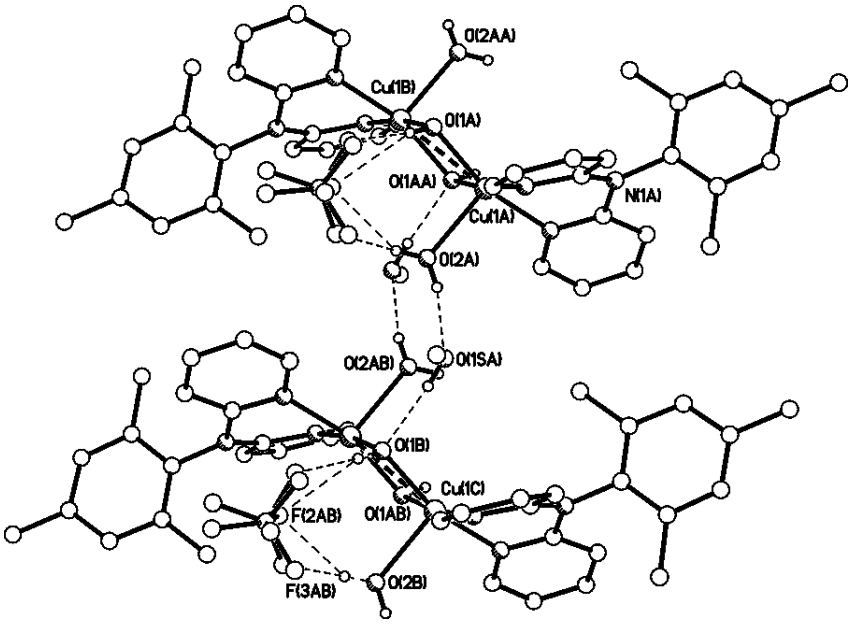

Fig. S11 Diagram of H-bonding network in **12** between copper-bound H_2O and OH^- ligands, MeOH solvent molecules, and BF_4^- anions. All hydrogen atoms attached to carbon are omitted for clarity.

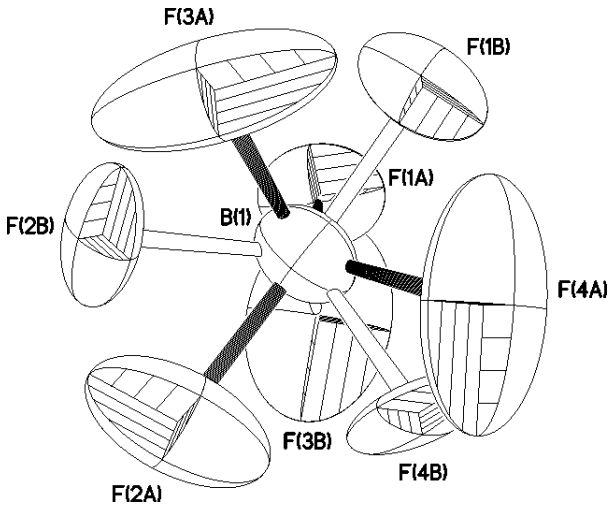

Fig. S12. Structure of the BF_4^- anion in compound **12** with both parts of the disorder present. For clarity, thermal ellipsoids are shown at the 20 % level.

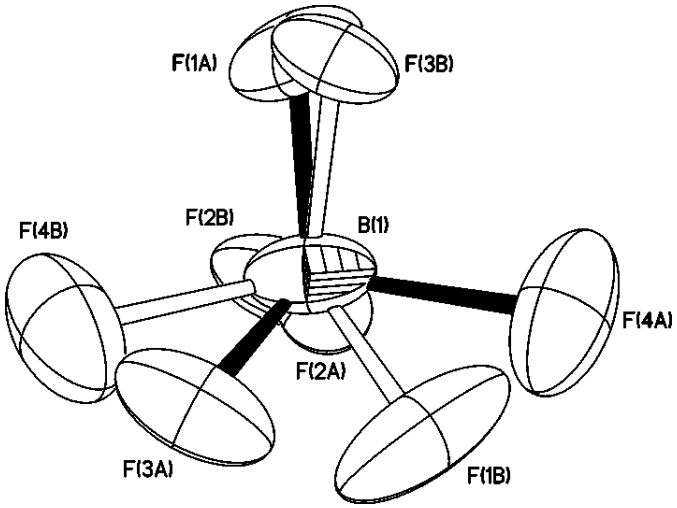

Fig. S13. Structure of the BF_4^- anion in compound **13** with both parts of the disorder present. Thermal ellipsoids are shown at the 30 % level.

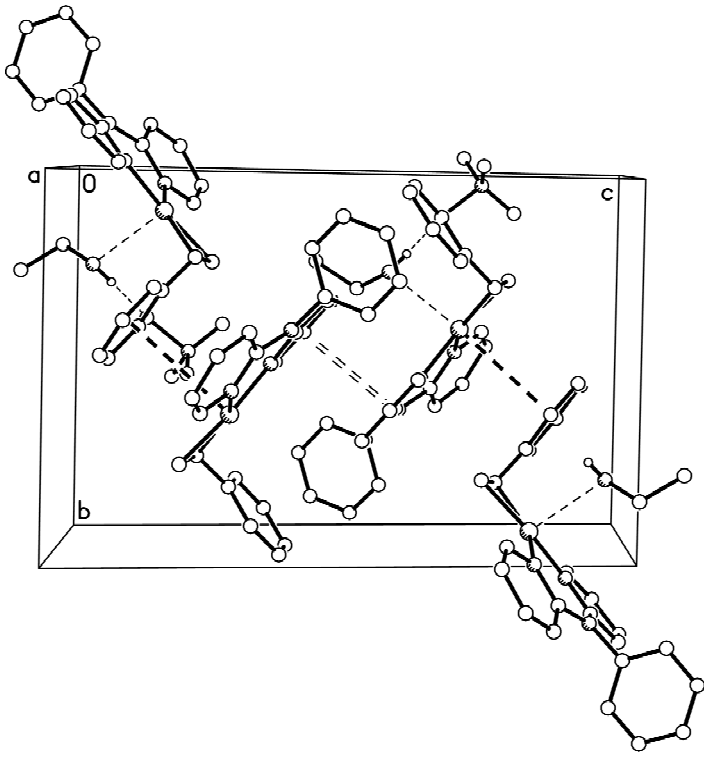

Fig. S14. Molecular packing diagram of **13** viewed along the a-axis, illustrating intermolecular interactions present in the lattice. Cu···Ph_{sty} π-interactions shown as thick dashed lines, π-π stacking between pyridyl rings shown as double-dashed line, Cu···O interactions and H-bonding between ethanol solvent molecule and BF_4^- anion shown as single thin dashed lines.

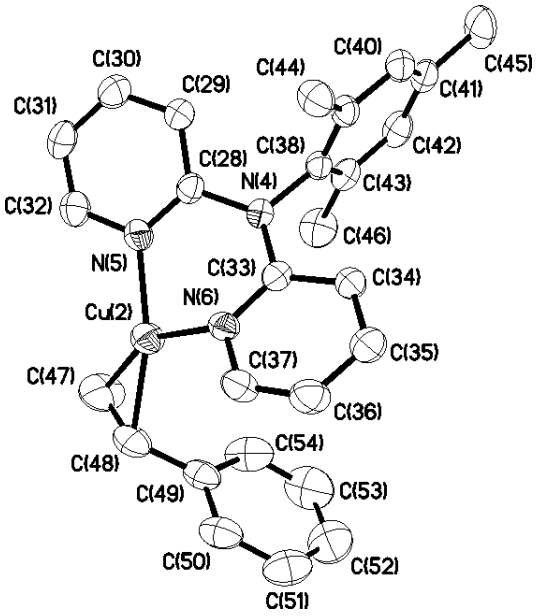

Fig. S15. Molecular structure of the second unique molecule present in the asymmetric unit of compound **14**. Thermal ellipsoids are shown at the 30% level, and all hydrogen atoms are omitted for clarity.

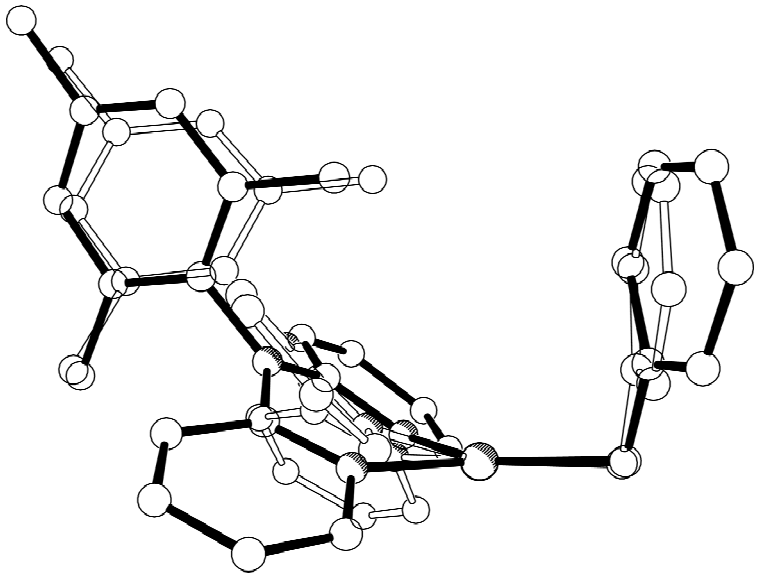

Fig. S16. Comparison of unique conformers present in the asymmetric unit of compound **14**.

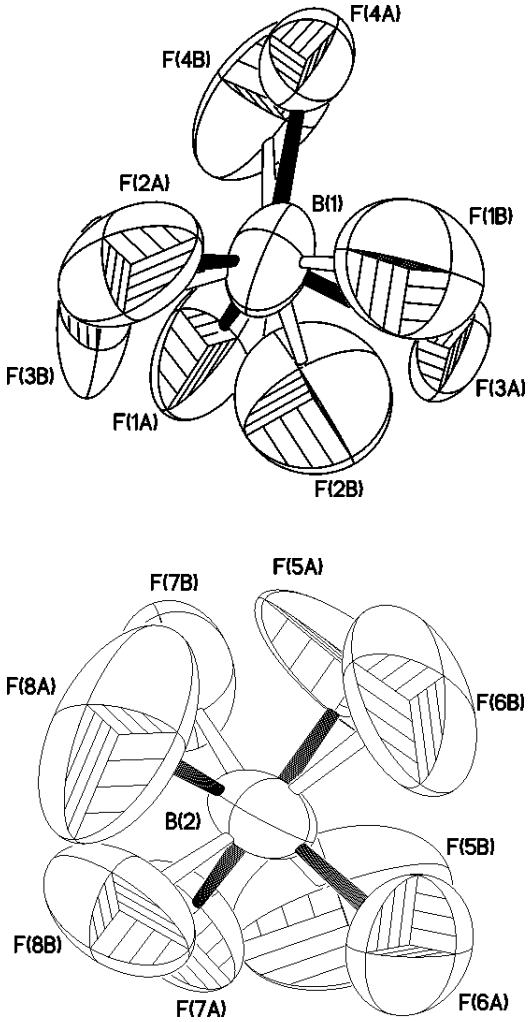

Fig. S17. Structure for the two disordered BF_4^- anions in compound **14** with both parts of the disorders present. For clarity, thermal ellipsoids are shown at the 20 % level.

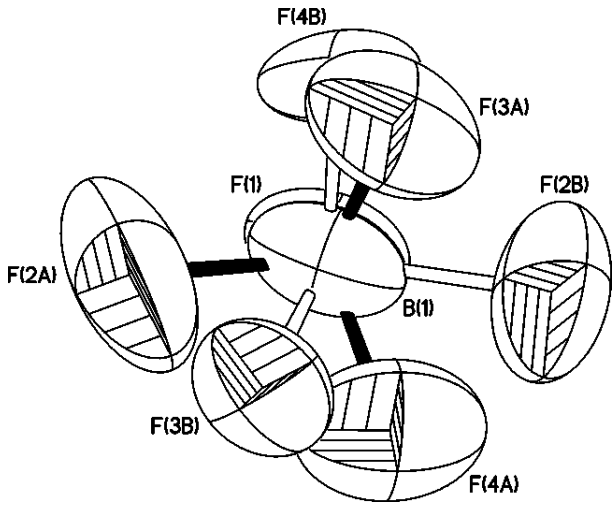

Fig. S18. Structure of the disordered BF_4^- anion in **15** with both parts of the disorder present. For clarity, thermal ellipsoids are shown at the 20 % level.

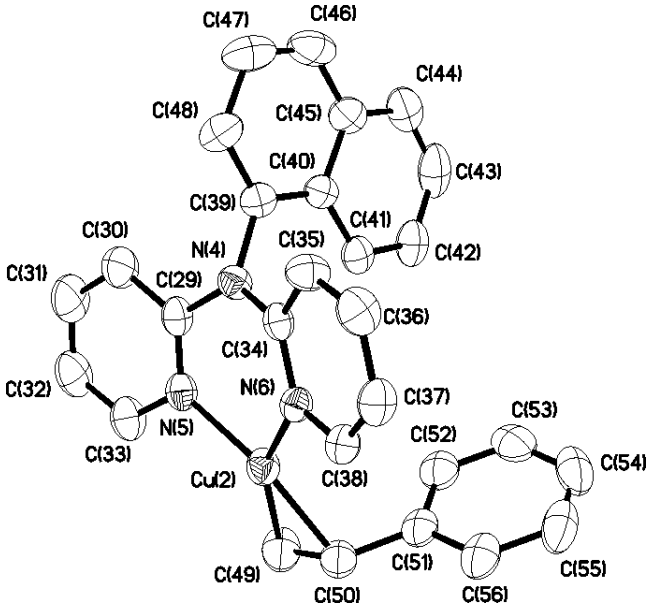

Fig. S19. Molecular structure of the second unique molecule present in the asymmetric unit of compound **16**. Thermal ellipsoids are shown at the 30% level, and all hydrogen atoms are omitted for clarity.

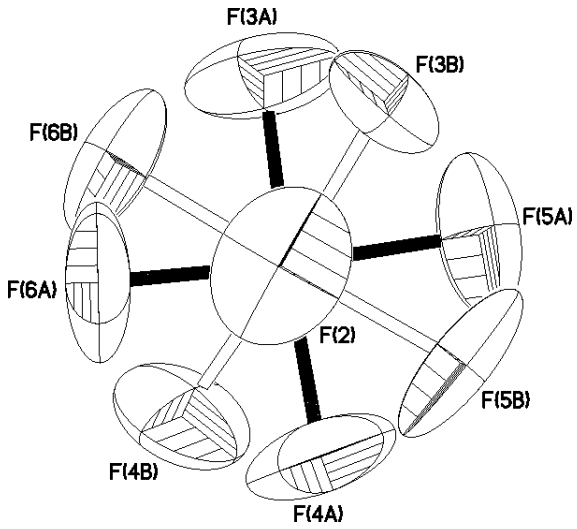

Fig. S20. Structure of the disordered PF_6^- anion in compound **17** with both parts of the disorder present. For clarity, thermal ellipsoids are shown at the 20 % level.

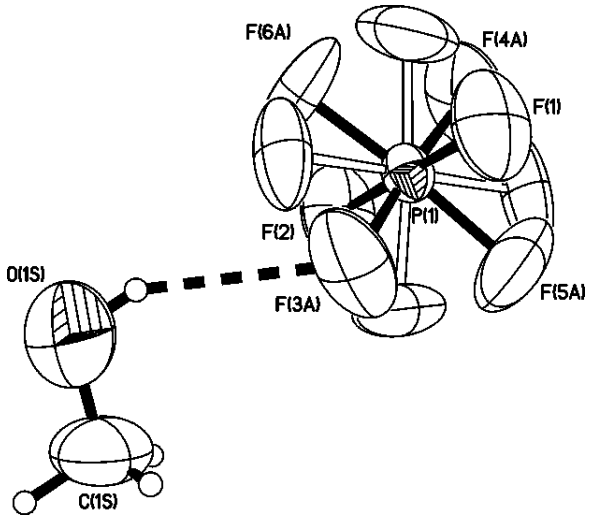

Fig. S21. H-bonding interaction in **17** between the PF_6^- anion and MeOH solvent molecule found to crystallize in the lattice. For clarity, thermal ellipsoids are shown at the 20 % level.